

# Dynamics of Aqueous Proline Solutions by Neutron Scattering and Molecular Dynamics Simulations

## Supporting Information

Paula Malo de Molina,<sup>1</sup> Fernando Alvarez,<sup>1,2</sup> Bernhard Frick,<sup>3</sup>  
Andrew Wildes,<sup>3</sup> Arantxa Arbe,<sup>1</sup> and Juan Colmenero<sup>1,2,4,\*</sup>

<sup>1</sup>*Centro de Física de Materiales (CFM) (CSIC–  
UPV/EHU) – Materials Physics Center (MPC),  
Paseo Manuel de Lardizabal 5, 20018 San Sebastián, Spain*

<sup>2</sup>*Departamento de Física de Materiales (UPV/EHU),  
Apartado 1072, 20080 San Sebastián, Spain*

<sup>3</sup>*Institut Laue-Langevin, 71 Avenue des Martyrs  
– CS 20156 – 38042 Grenoble Cedex 9, France*

<sup>4</sup>*Donostia International Physics Center,  
Paseo Manuel de Lardizabal 4, 20018 San Sebastián, Spain*

---

\* [juan.colmenero@ehu.eus](mailto:juan.colmenero@ehu.eus)

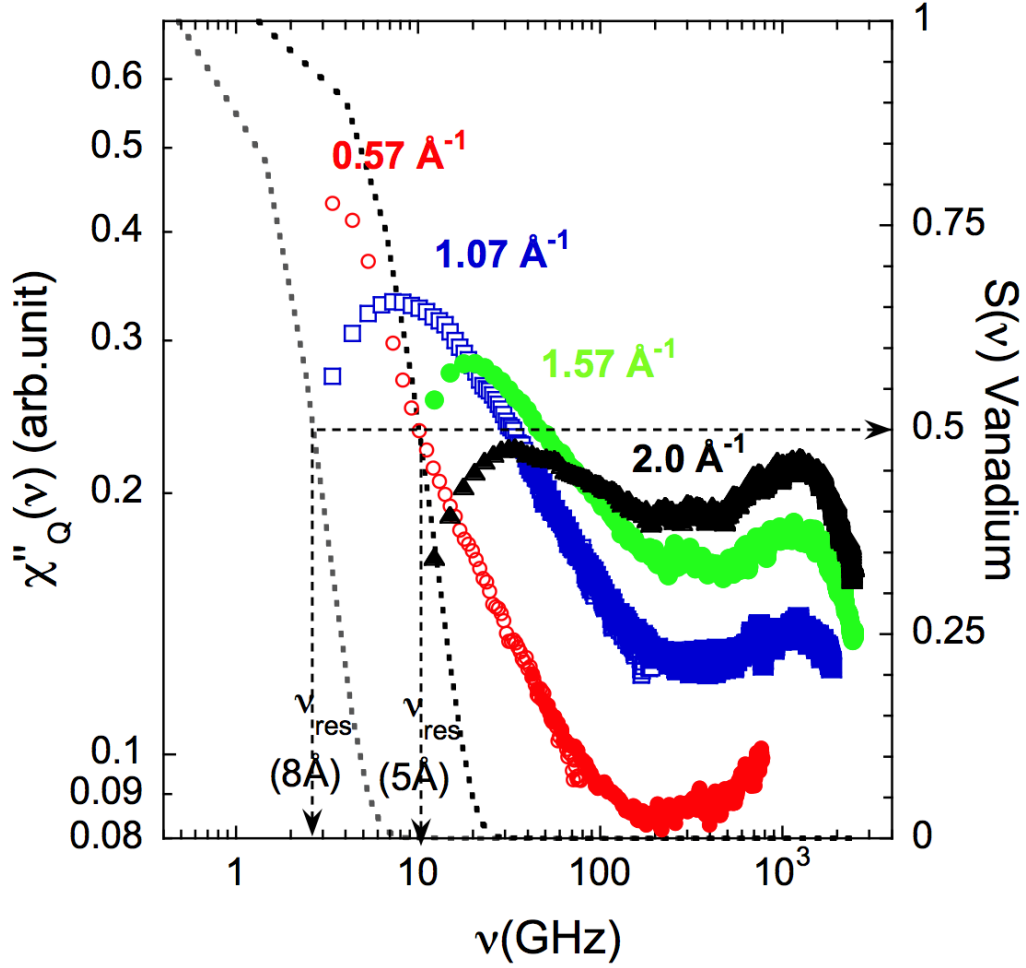


FIG. S1. Imaginary part of the susceptibility obtained from the IN5 spectra (empty symbols: from  $8 \text{ \AA}$ , full symbols, from  $5 \text{ \AA}$ ) for the sample  $6\text{H}_2\text{O}$  shown in Fig. S2(b) and (c). The resolution functions (Vanadium spectra) are also shown for comparison (dotted curves), with the dotted lines marking the resolution frequencies determined by the HWHM. The data corresponding to  $0.57 \text{ \AA}^{-1}$ , where no clear maximum is observed for the diffusive process, were not fitted by the model. In the other cases, where the maximum attributable to diffusion is clearly resolved at frequencies higher than  $\nu_{res}$ , the model was applied.

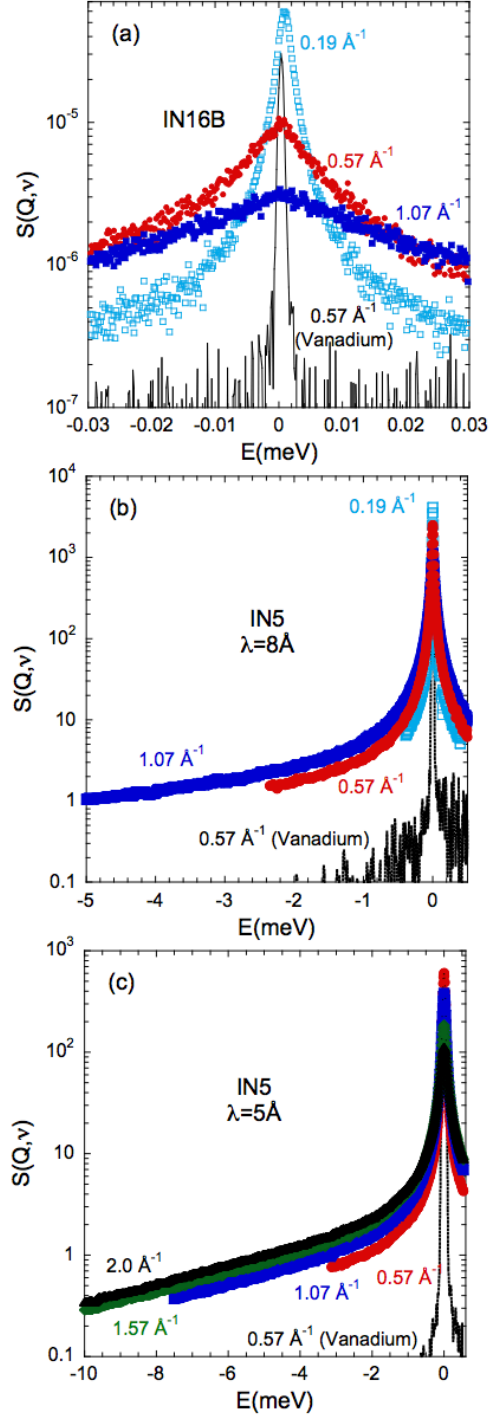


FIG. S2. QENS spectra of a D-proline solution in  $H_2O$  with  $x = 6$  measured with the instruments IN16B (a) and IN5 with wavelengths  $\lambda = 5$  (b) and  $8 \text{ \AA}$  (c) at different  $Q$ -values compared to the instrument resolution (line).

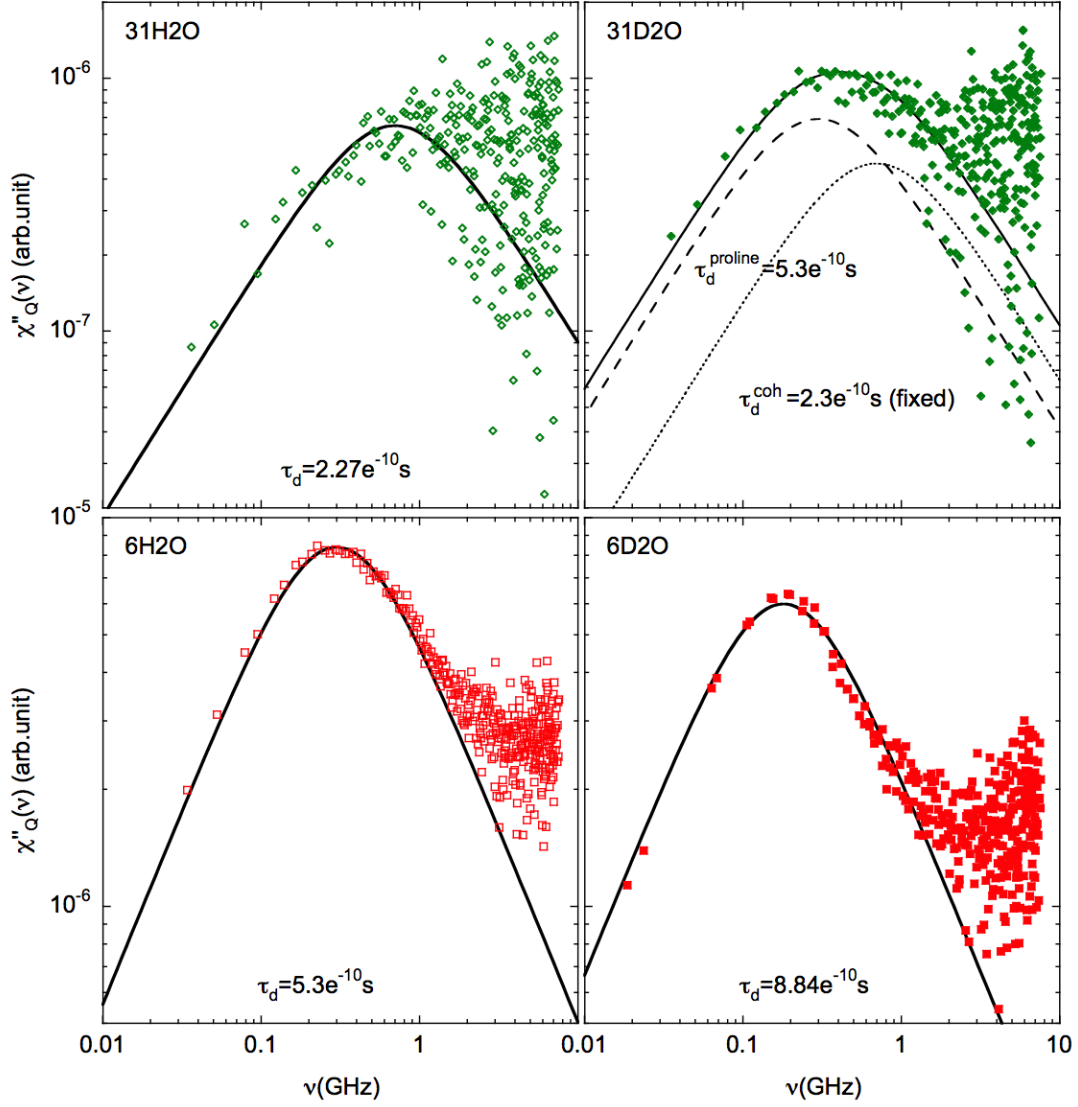


FIG. S3. Susceptibility of all samples measured on IN16B at  $Q = 0.19 \text{ \AA}^{-1}$ . Lines are fits of Debye functions to the peak region and low-frequency flank of the spectra. For the 31D2O sample, Eq. 13 has been applied where  $\tau_d^{\text{coh}}$  has been fixed, as a first approach, to the incoherent value obtained for the water component from the analysis of the 31H<sub>2</sub>O sample.

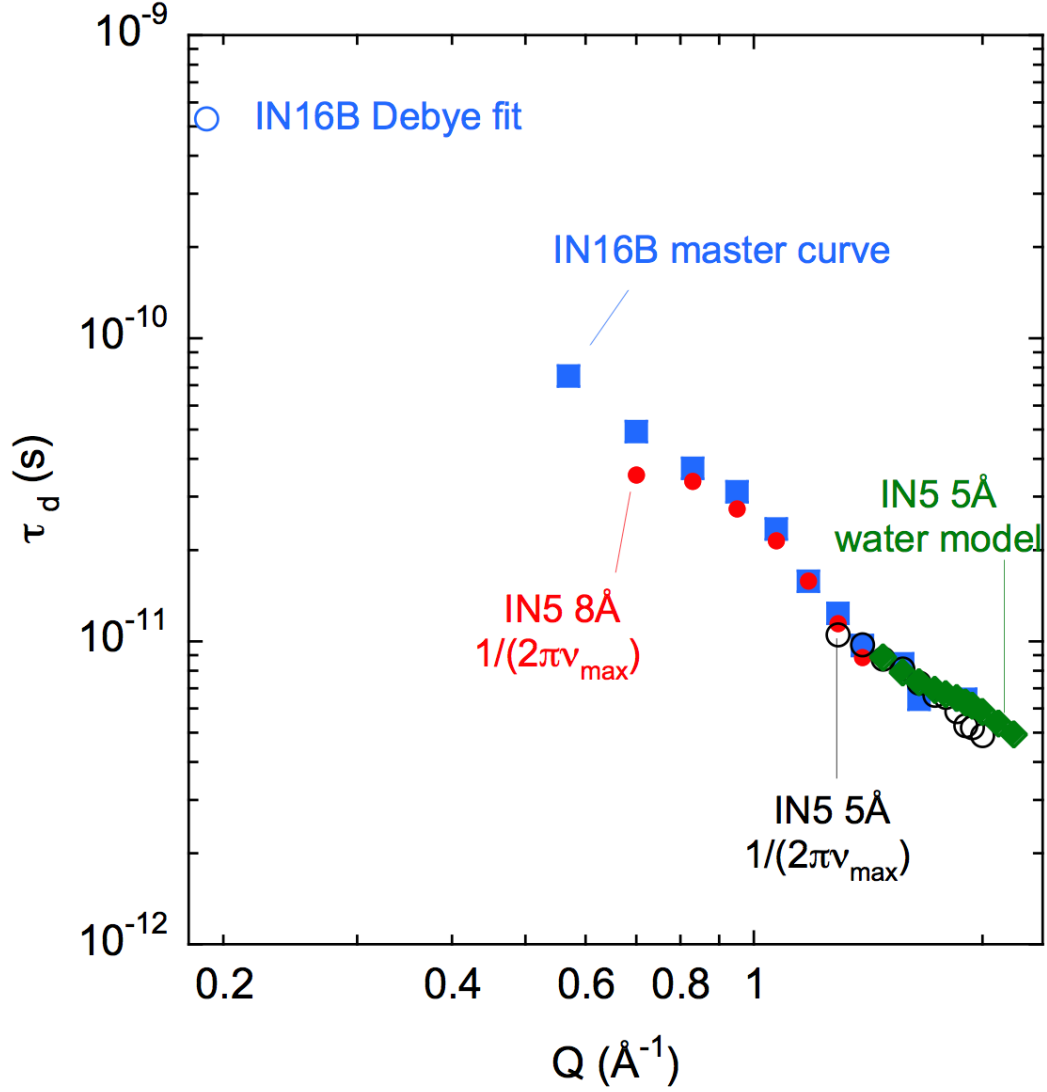


FIG. S4. Diffusive time  $\tau_d$  of the sample  $6\text{H}_2\text{O}$  obtained from fitting the water model to the high- $Q$  spectra (Figure 2), from the low frequency maxima as  $\tau_d = 1/(2\pi\nu_{max})$ , from the shift factors used in the construction of a master curve from the IN16B results (Figure S5) and from the fit to a single Debye process to IN16B data at  $Q = 0.19 \text{ \AA}^{-1}$  data (Figure S3).

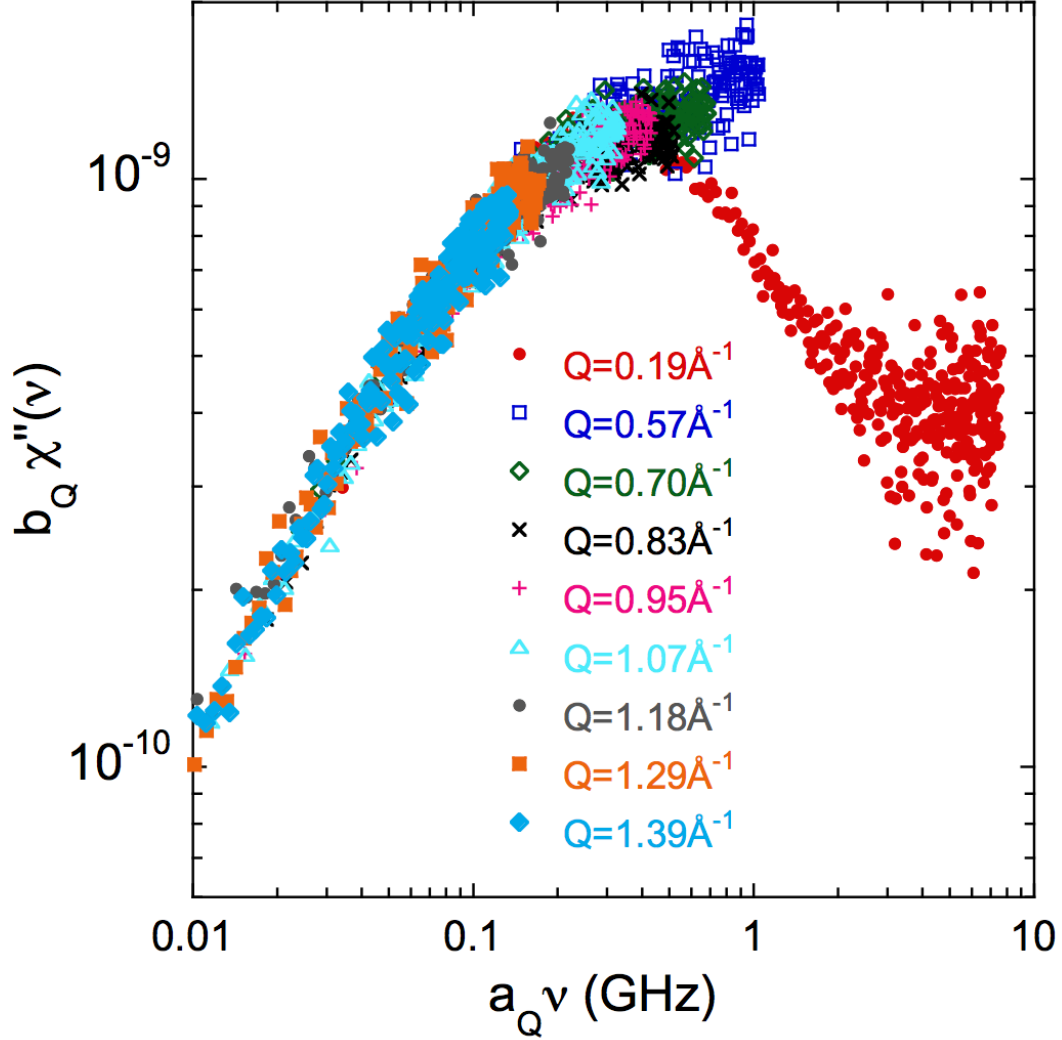


FIG. S5. Master curve constructed from the susceptibility measured by IN16B on the  $6\text{H}_2\text{O}$  sample at 298 K, applying  $Q$ -dependent amplitude factors  $b_Q$  and frequency shift factors  $a_Q$  (Reference  $Q = 0.19 \text{ \AA}^{-1}$ ). In this case, as in the other master curves constructed, there was no systematic dependence observed for the  $b_Q$ -factors, which were scattered around unity. The obtained superposition is good in the low-frequency regime –which is the relevant one to extract the information about the  $Q$ -dependence of the diffusive process–. We note the relatively high scattering of the experimental data at high frequencies, that might hamper resolving the maximum of the diffusive component of the susceptibility (mainly in the data corresponding to  $Q \approx 0.57 \text{ \AA}^{-1}$ , where it would be expected to be present). These observations also apply to the master curves shown in other figures.

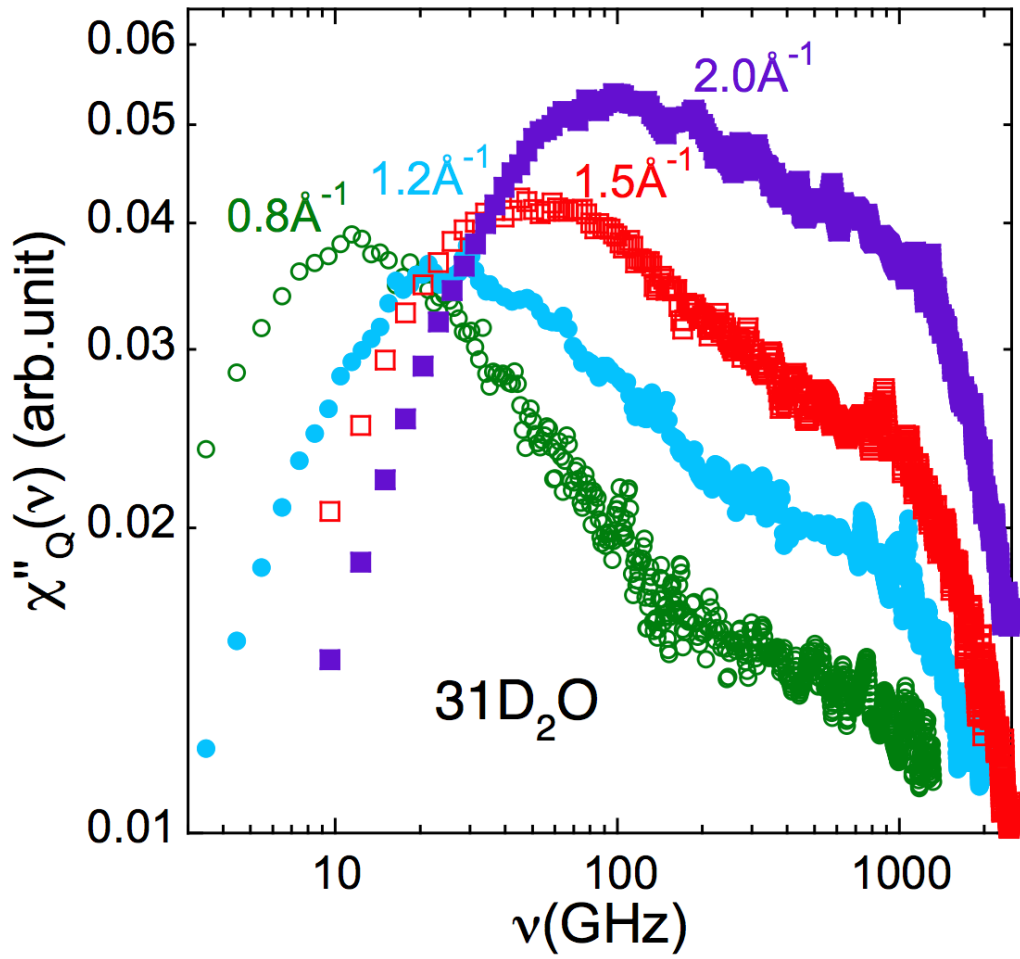


FIG. S6. Imaginary part of H-proline/D<sub>2</sub>O solution with  $x=31$  at the different  $Q$ -values indicated.

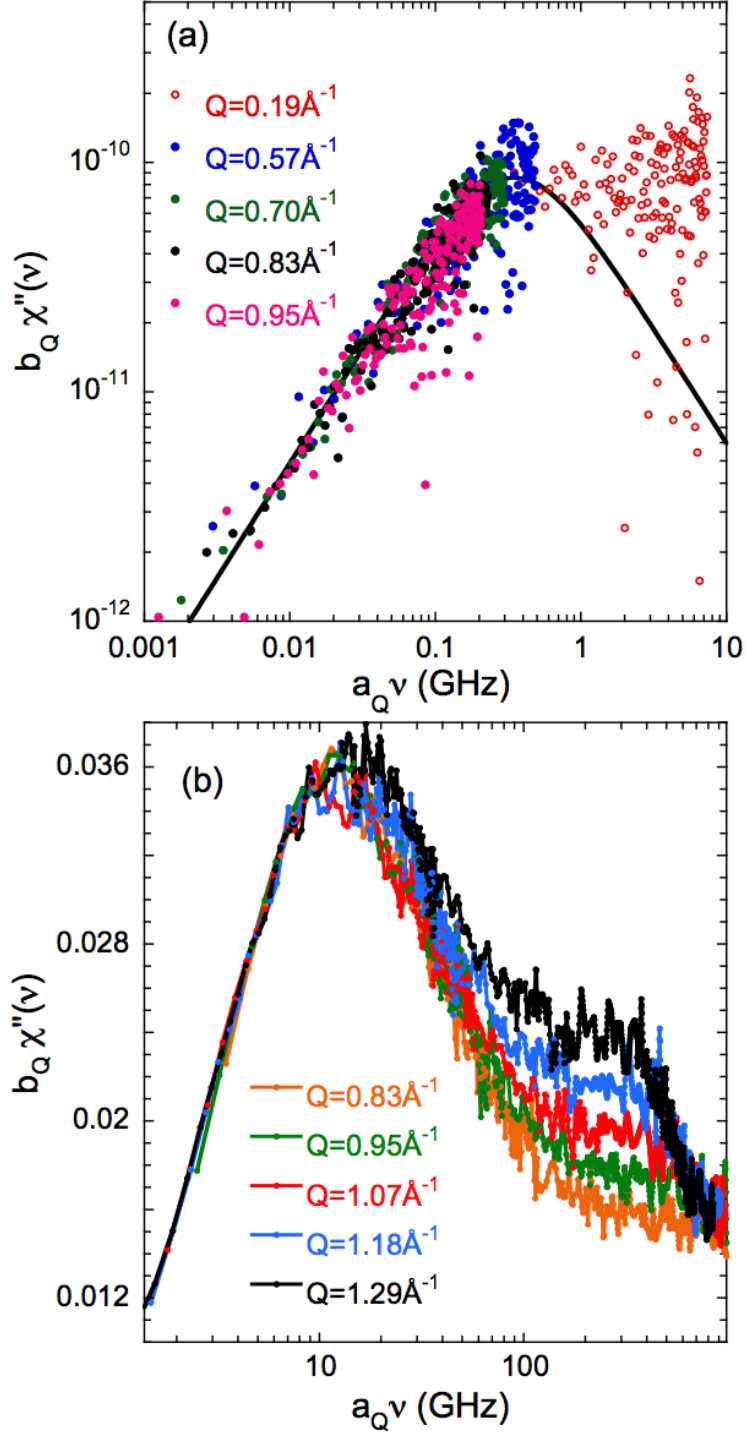


FIG. S7. Master curves constructed from the susceptibility measured on the  $31\text{D}_2\text{O}$  sample at 298 K, applying  $Q$ -dependent amplitude factors  $b_Q$  and frequency shift factors  $a_Q$ . Results in (a) correspond to IN16B measurements (Reference  $Q = 0.19 \text{ \AA}^{-1}$ ) and in (b) to IN5 experiments (8  $\text{\AA}$ ) (Reference  $Q = 0.83 \text{ \AA}^{-1}$ ).



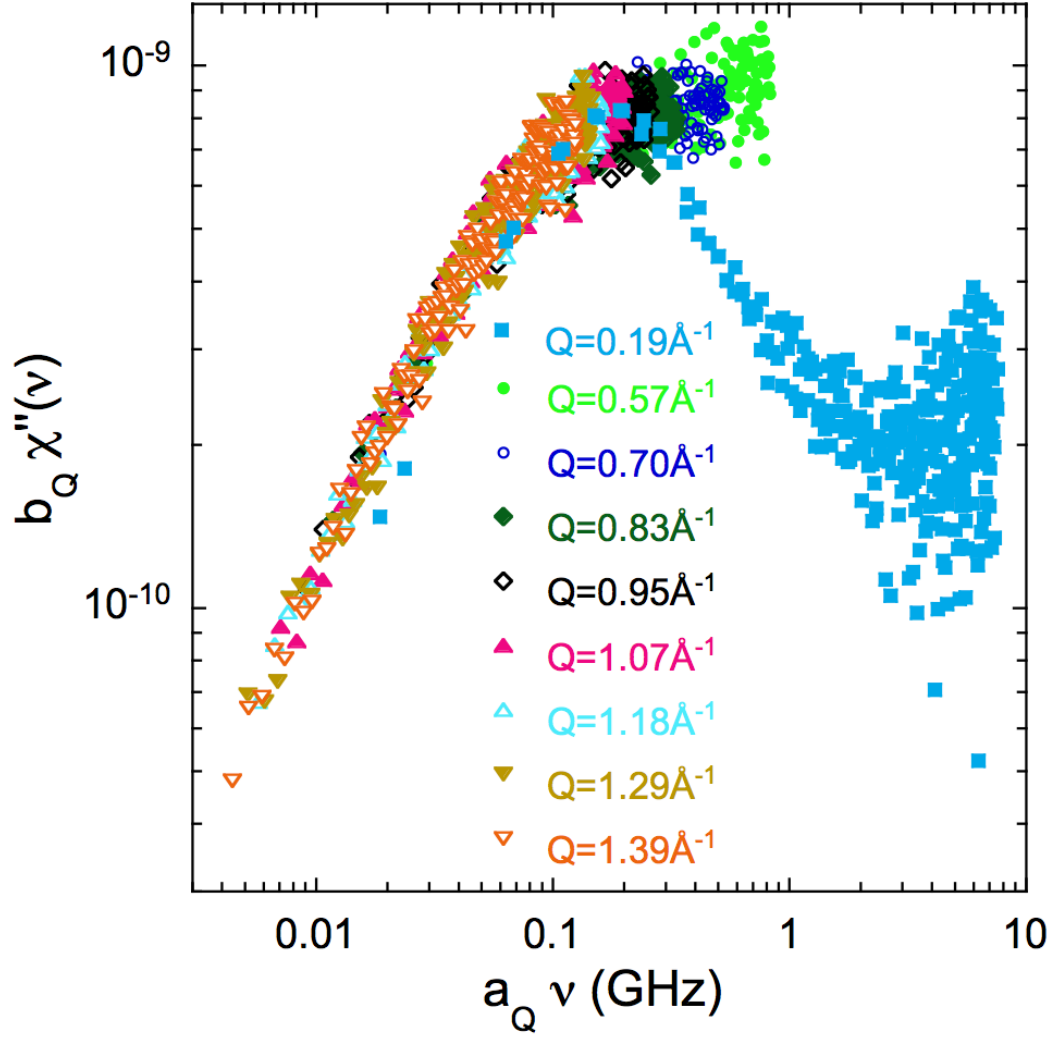


FIG. S8. Master curve constructed from the susceptibility measured by IN16B on the  $6\text{D}_2\text{O}$  sample at 298 K, applying  $Q$ -dependent amplitude factors  $b_Q$  and frequency shift factors  $a_Q$  (Reference  $Q = 0.19 \text{ \AA}^{-1}$ ).

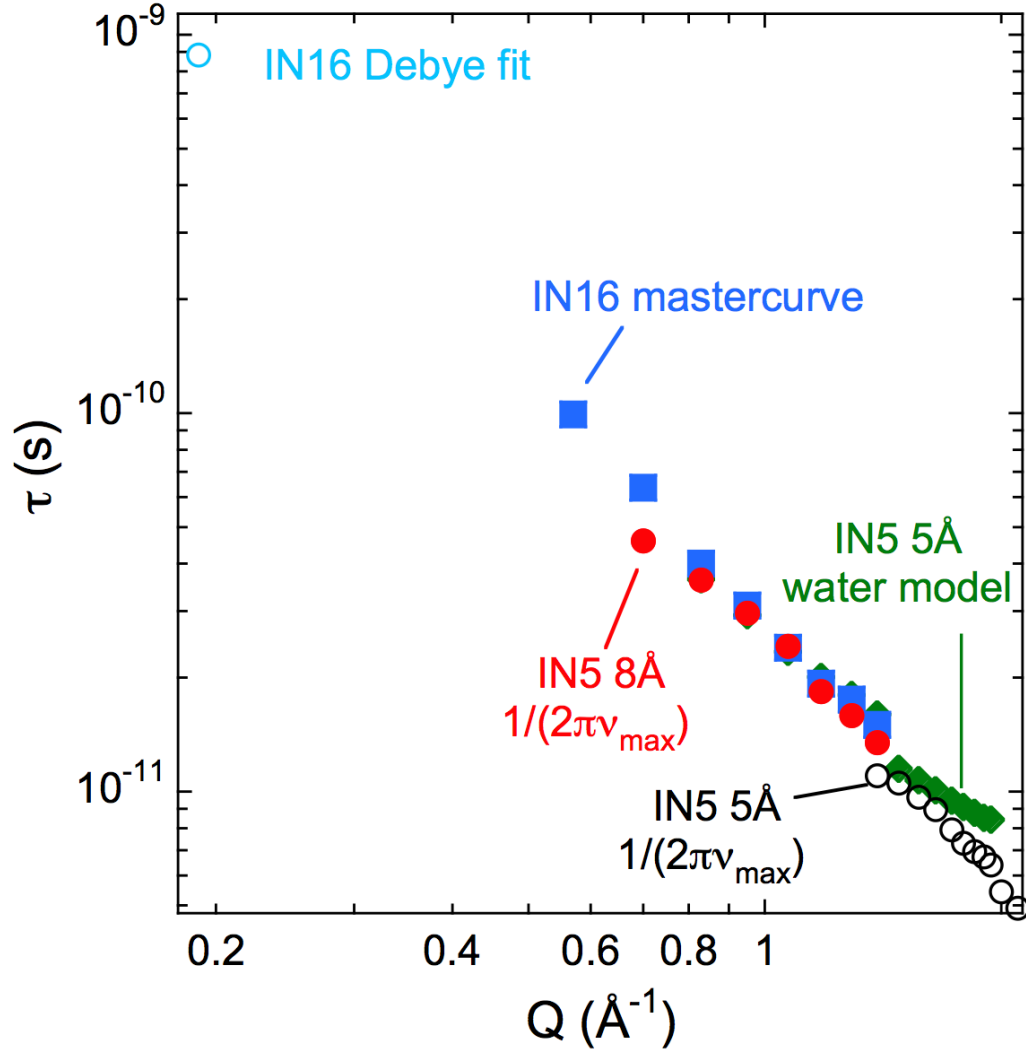


FIG. S9. Diffusive time  $\tau_d$  of the sample  $6\text{D}_2\text{O}$  obtained from fitting the water model to the high- $Q$  spectra (Figure 6), from the low frequency maxima as  $\tau_d = 1/(2\pi\nu_{\max})$ , from the shift factors used in the construction of a master curve from the IN16B results (Figure S8) and from the fit to a single Debye process to IN16B data at  $Q = 0.19 \text{ \AA}^{-1}$  data (Figure S3).

## Analysis of the Temperature Dependence

The temperature dependence of the component dynamics was investigated for the concentrated solution. For  $T < 300$  K the diffusive component became too slow to be well resolved by IN5. Therefore, for each sample, the temperature dependence of the diffusive component was determined from the IN16B results in the following way: first, for a given temperature, master curves were obtained applying  $Q$ -dependent shift factors; thereafter, a single master curve was built using  $T$ -dependent shift factors to superimpose the former masters. Figure S10 shows the finally obtained master curve for the 6H<sub>2</sub>O sample. From this construction we obtained the  $T$ -dependent shift factors governing the diffusive component ( $\tau_d$ ). To obtain the  $T$ -dependences of the characteristic times of the other processes, we applied the bulk-water-like model to the high- $Q$  IN5 data (i. e.,  $Q=1.8 \text{ \AA}^{-1}$ ) –where this model provides a good description of the experimental data. In the fitting procedure we fixed the value of  $\tau_d(Q=1.8 \text{ \AA}^{-1}, T)$  to the value obtained for  $\tau_d(Q=1.8 \text{ \AA}^{-1}, T = 298 \text{ K})$  affected by the previously obtained  $T$ -dependent shift factors. Some representative examples of the descriptions of the susceptibilities obtained in this way are shown in Fig. S11. The quality of the fits can be considered as reasonable given that the diffusive time has been fixed and considering the resolution influence in the lowest temperature data. The values of the  $b_Q$  factors applied to the amplitudes of the data were scattered around 1.

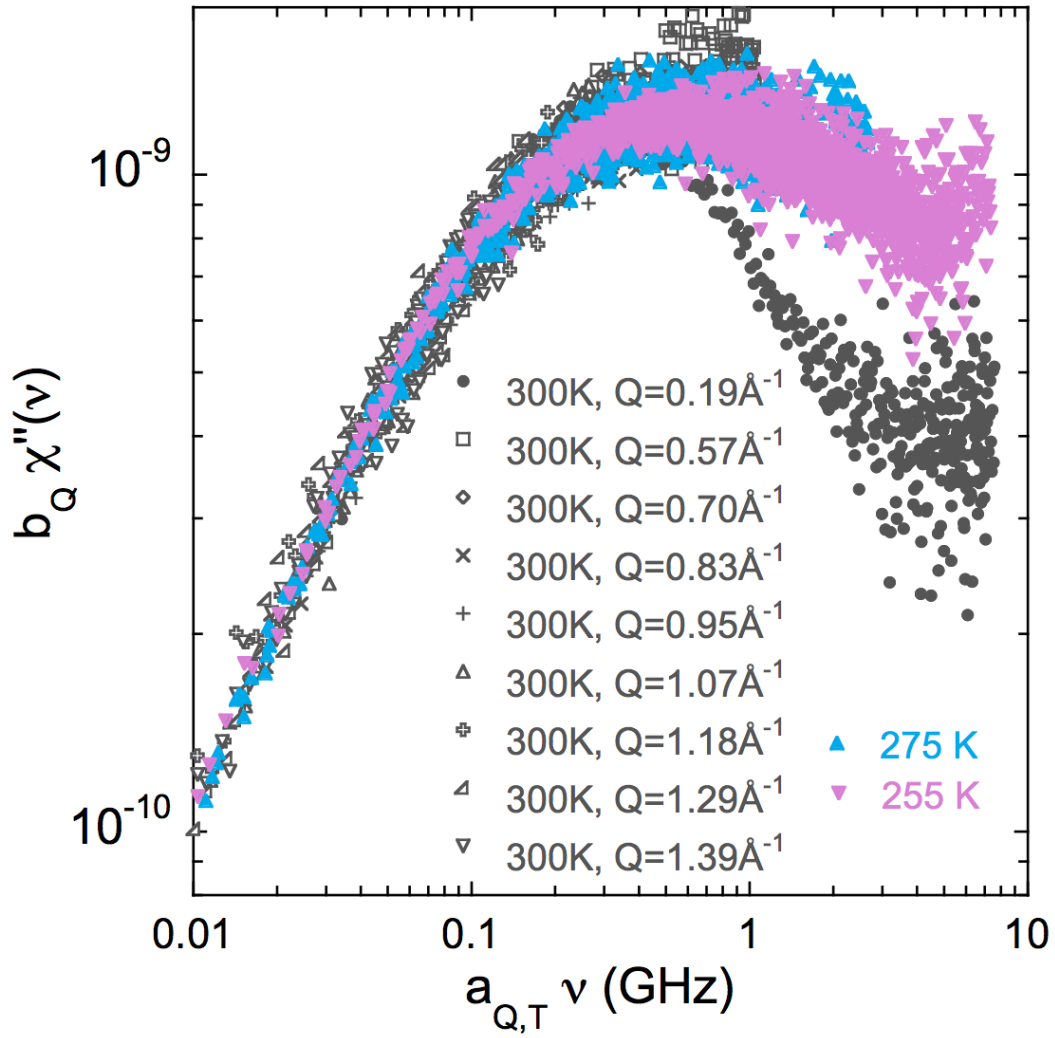


FIG. S10. Temperature, scattering vector and time superposition curve for the  $6\text{H}_2\text{O}$  sample susceptibility measured by IN16B. The reference  $Q$  and temperature are  $0.19\text{ \AA}^{-1}$  and  $298\text{ K}$ , respectively.

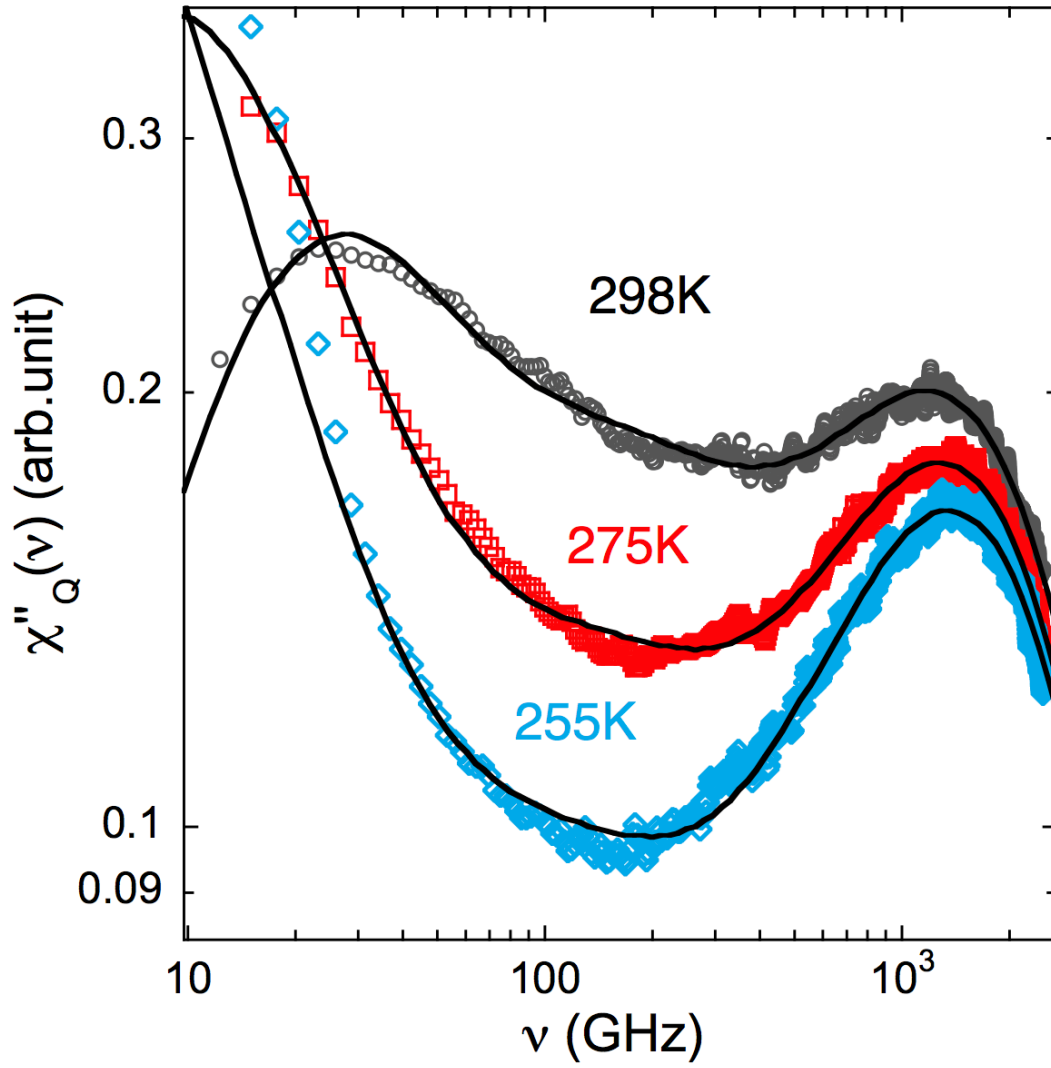


FIG. S11. Susceptibility curves obtained from the ToF results on the  $6\text{H}_2\text{O}$  sample at  $Q = 1.8 \text{ \AA}^{-1}$  and the temperature values indicated. Solid lines are fits of the convolution model function.

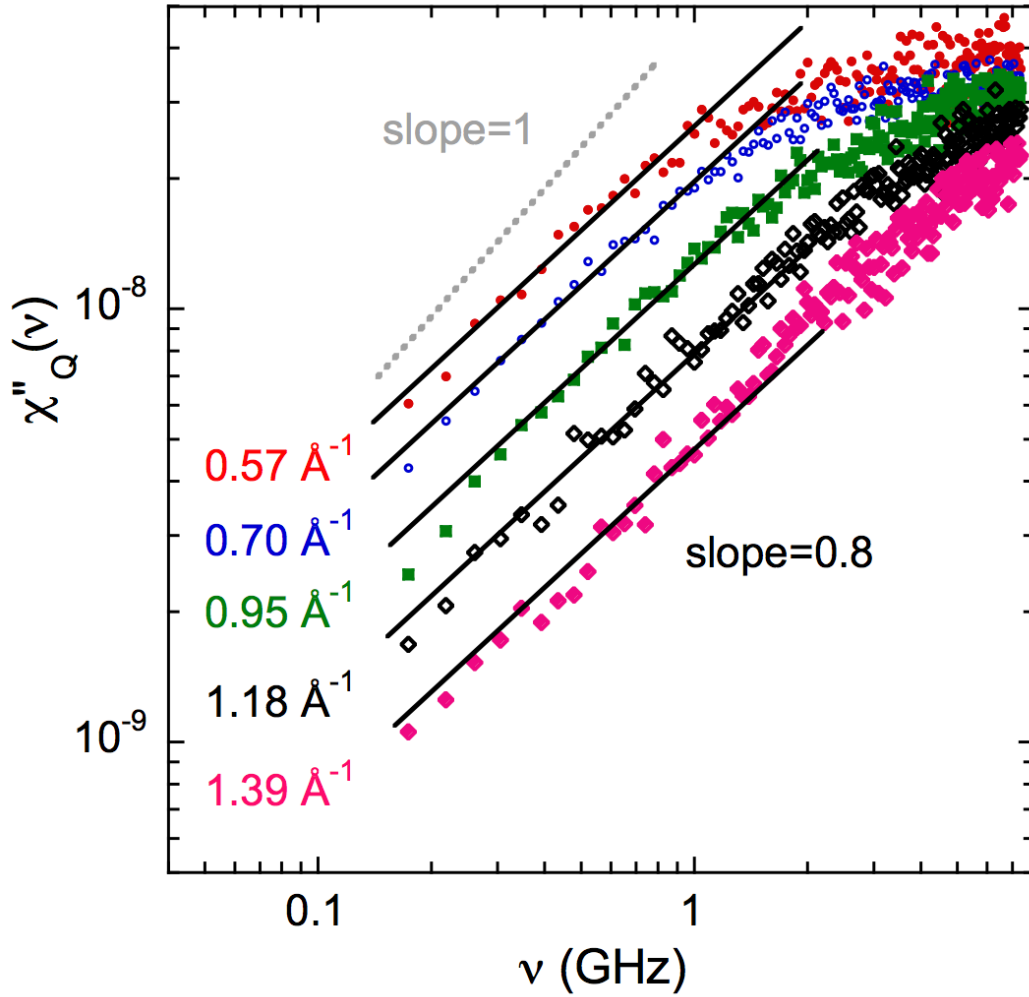


FIG. S12. Susceptibility curves obtained from the backscattering results on the  $6\text{H}_2\text{O}$  sample at 298 K and the  $Q$ -values indicated. For a Cole-Cole functional form, the slope of the low-frequency flank of the imaginary part of the susceptibility has an asymptotic value determined by the shape parameter  $\gamma$  ( $\chi''(\nu \ll 1/\tau) \propto \nu^\gamma$ ). Solid lines have a slope of 0.8; dotted line shows a slope of 1 (Lorentzian case).